BIOCHEMISTRY
including biophysical chemistry & molecular biology

Article

pubs.acs.org/biochemistry

Structural Characterization of HP1264 Reveals a Novel Fold for the Flavin Mononucleotide Binding Protein

Ki-Young Lee, Ji-Hun Kim,† Kyu-Yeon Lee, Jiyun Lee, Ingyun Lee, Ye-Ji Bae, and Bong-Jin Lee*

Research Institute of Pharmaceutical Sciences, College of Pharmacy, Seoul National University, Seoul 151-742, Korea

Supporting Information

ABSTRACT: Complex I (NADH-quinone oxidoreductase) is an enzyme that catalyzes the initial electron transfer from nicotinamide adenine dinucleotide (NADH) to flavin mononucleotide (FMN) bound at the tip of the hydrophilic domain of complex I. The electron flow into complex I is coupled to the generation of a proton gradient across the membrane that is essential for the synthesis of ATP. However, *Helicobacter pylori* has an unusual complex I that lacks typical NQO1 and NQO2 subunits, both of which are generally included in the NADH dehydrogenase domain of complex I. Here, we determined the solution structure of HP1264, one of the unusual subunits of complex I from *H. pylori*, which is located in place of NQO2, by three-dimensional nuclear magnetic resonance (NMR) spectroscopy and revealed that HP1264 can bind to FMN through UV−visible, fluorescence, and NMR titration experiments. This result suggests that FMN-bound HP1264 could be involved in the initial electron transfer step of complex I. In addition, HP1264 is structurally most similar to *Escherichia coli* TusA, which belongs to the SirA-like superfamily having an IF3-like fold in the SCOP database, implying that HP1264 adopts a novel fold for FMN binding. On the basis of the NMR titration data, we propose the candidate residues Ile32, Met34, Leu58, Trp68, and Val71 of HP1264 for the interaction with FMN. Notably, these residues are not conserved in the FMN binding site of any other flavoproteins with known structure. This study of the relationship between the structure and FMN binding property of HP1264 will contribute to improving our understanding of flavoprotein structure and the electron transfer mechanism of complex I.

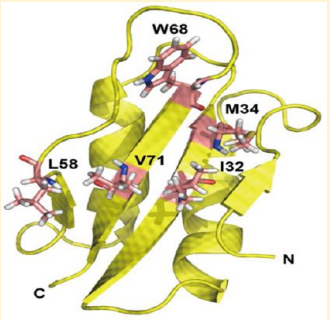

FMN-binding site of HP1264

Helicobacter pylori is a human pathogenic bacterium that is found in the stomach of more than 50% of the world's population. This bacterium is supposed to be related to the development of diverse duodenogastric diseases such as chronic gastritis, peptic ulcers, duodenal ulcers, stomach cancer, etc.[1−3] Over the past few decades, multiple antibiotic therapies have been used in treating *H. pylori* infections. Unfortunately, they have been accompanied by the global prevalence of *H. pylori* resistance to various antibiotics, which has been an emerging issue in the 21st Century.[4,5] Therefore, much effort has been focused on discovering new antibiotic drug candidates for *H. pylori* infections. Recently, a database of *H. pylori* essential genes for cell viability has been established, providing useful information in the search for excellent targets for new antibiotic drugs.[6] On the basis of this database, several complex I subunits from *H. pylori* are now regarded as essential proteins needed for cell growth and maintenance. In particular, HP1264, also known as complex I subunit E from *H. pylori*, is categorized as one of the essential proteins.

Complex I (NADH-quinone oxidoreductase) is one of the largest known membrane protein complexes. In mitochondria and many bacteria, the enzyme catalyzes the transfer of two electrons from cytosolic NADH to FMN bound at the tip of the peripheral hydrophilic arm of complex I.[7,8] The reduced enzyme then passes the electrons through the iron−sulfur (Fe−S) clusters to ubiquinone at the interface between the hydrophilic and membrane domains of complex I. This electron transfer is coupled to the translocation of four protons across the membrane, providing ∼40% of the proton flux during proton-motive force (PMF) generation for the synthesis of ATP.[9−12] However, it has been reported that, in human mitochondria, complex I also has detrimental effects on cell survival by producing reactive oxygen species (ROS), which can lead to mitochondrial DNA damage causing aging and neurodegenerative diseases such as Parkinson's disease, Alzheimer's disease, etc.[13,14]

The core subunits of complex I are highly conserved from bacteria to humans; thus, bacterial complex I can represent a minimal model of eukaryotic mitochondrial complex I.[9,10,12,15] Previously, the overall structure of bacterial complex I in several redox states has been determined by X-ray crystallography or electron microscopy.[16−21] The crystal structure of complex I from *Thermus thermophilus* adopts an L-shaped architecture that is composed of 15 core subunits (eight hydrophilic and seven hydrophobic domains) with a combined molecular mass of ∼550 kDa. The hydrophobic subunits are embedded in the cell membrane, and the hydrophilic subunits protrude into the cytosol. In general, each subunit contained in the hydrophilic domain has more than one iron−sulfur (Fe−S) cluster. The redox components, Fe−S clusters and FMN, communicate with each other and cooperatively relay electrons across complex

Received: December 29, 2012
Revised: February 12, 2013
Published: February 13, 2013

   dx.doi.org/10.1021/bi301714a | *Biochemistry* 2013, 52, 1583−1593

I.[16,21] Especially, FMN plays a central role as a cofactor of complex I by the nature of its primary electron acceptor from NADH. On the other hand, reduced forms of FMN, flavosemiquinone and $FMNH_2$, can generate a harmful ROS by the reduction of oxygen.[22] On the basis of the crystal structure of complex I from *T. thermophilus,* the FMN binding property of complex I has been shown to be attributed to a Rossmann fold-like domain adopted by the NQO1 subunit.[16]

In *H. pylori*, a gene cluster of complex I has been identified and hypothesized to encode the combination of seven hydrophilic and seven hydrophobic subunits like many bacteria. However, structural and biochemical studies of these individual subunits have not been extensively conducted until now. Of these complex I subunits, we studied HP1264 annotated as complex I subunit E from *H. pylori* for the following reasons. (i) HP1264 could be one of the probable antibiotic drug targets from *H. pylori*, and (ii) the unique sequence of HP1264 suggests its unusual biological implications. Here, we show that HP1264 can bind to FMN using UV−visible absorption, fluorescence quenching, and NMR chemical shift experiments. We also determined the solution structure of HP1264 and its possible FMN binding residues by NMR spectroscopy and discovered that HP1264 has a novel fold for FMN binding.

MATERIALS AND METHODS

Protein Expression and Purification. The HP1264 gene was acquired from the *H. pylori* genomic DNA by PCR amplification and subcloned into the plasmid pET21a (Novagen Inc.). This plasmid was transformed into *Escherichia coli* BL21 (DE3) host cells. HP1264 was expressed as a fusion protein with eight non-native residues that correspond to a hexahistidine tag (LEHHHHHH) at the C-terminus. Overexpression was induced with 0.5 mM isopropyl β-D-thiogalactopyranoside (IPTG) at 37 °C for 4 h. Cells were sonicated in lysis buffer, which consisted of 50 mM Tris-HCl buffer (pH 8.0) and 500 mM NaCl. The protein was purified using His_6 tag affinity chromatography (Chelating Sepharose Fast Flow resin, Pharmacia) and gel filtration (Superdex 75 10/300, Amersham Biosciences) with the AKTA prime system (Amersham). FMN-free HP1264 was prepared by using the following steps: trichloroacetic acid precipitation, washing the FMN-free precipitate, and redissolving the apoprotein in buffer.[23] Uniformly ^{15}N- and ^{13}C-labeled protein was prepared by growing the cells in M9 medium, which contained 99% $^{15}NH_4Cl$ and 99% [^{13}C]-D-glucose (Cambridge Isotopes). The NMR sample was prepared at a concentration of ~1 mM in a 90% H_2O/10% D_2O mixture containing 20 mM NaH_2PO_4/Na_2HPO_4 buffer (pH 6.0) and 150 mM NaCl.

UV−Visible Absorption Spectroscopy. UV−visible absorption spectra were recorded with the NanoDrop ND-1000 spectrophotometer (NanoDrop Tech, Wilmington, DE). Spectra were recorded for free FMN (20 μM) without and with an increasing amount of FMN-free HP1264 (40, 80, and 120 μM). All titration buffer conditions were maintained at 25 °C in 20 mM NaH_2PO_4/Na_2HPO_4 buffer (pH 6.0) containing 150 mM NaCl.

Fluorescence Spectroscopy. Fluorescence spectra were obtained with the SpectraMax Gemini XS Microplate Fluorometer. In FMN fluorescence titration experiments, purified apo-HP1264 (0.04−2 mM) and free FMN/NADH (0.4 mM) were used. The excitation and emission wavelengths of FMN were 435 and 528 nm, respectively, and the excitation and emission wavelengths of NADH were 341 and 460 nm, respectively. In titration experiments aimed at the tryptophan fluorescence of HP1264, purified apo-HP1264 (0.1 mM) and FMN (0.01−0.5 mM) were used. The excitation and emission wavelengths of tryptophan of HP1264 were 280 and 330 nm, respectively. In all cases, we selected the best excitation wavelength after scanning the excitation wavelengths giving a maximal fluorescence signal. All samples for measurements were always prepared with 20 mM NaH_2PO_4/Na_2HPO_4 buffer (pH 6.0) containing 150 mM NaCl and incubated for 10 min at 25 °C before the fluorescence signals were collected. Corrections for background fluorescence changes were made by titrations with buffer.

NMR Measurements and Structure Determination. All NMR experiments were performed at 298 K on a Bruker AVANCE DRX 600 spectrometer equipped with a cryogenic probe and a Bruker AMX 500 spectrometer. Backbone and side chain peak assignments were performed using a series of triple-resonance spectra [three-dimensional (3D) HNCO, HN(CA)-CO, HNCA, HN(CO)CA, HNCACB, HN(CO)CACB, HBHA(CO)NH, HCCH-TOCSY, C(CO)NH, and HC(CO)-NH]. Aromatic ring proton resonances were assigned using two-dimensional (2D) NOESY, 3D ^{15}N NOESY-HSQC, and 3D ^{13}C NOESY-HSQC. Chemical shifts were referenced to DSS externally. NMR data were processed using NMRPipe[24] and analyzed with NMRView.[25] The distance restraints for the structure calculation were collected from the 3D ^{15}N NOESY-HSQC and ^{13}C NOESY-HSQC spectra by manual and automatic assignments for which CYANA 2.1 was used.[26] Dihedral angle restraints were calculated from the chemical shifts using TALOS,[27] and the overall secondary structure was predicted from the chemical shift index (CSI)[28] and NOE pattern. Hydrogen bond restraints were obtained using the H−D exchange experiment and observation of regular secondary structure elements from the CSI search and NOE patterns. The structures were initially generated with CYANA 2.1 and then refined through standard annealing and torsion angle dynamics using CNS version 1.3.[29] MOLMOL and PyMOL (DeLano Scientific LLC) were used to visualize the result of 20 energy-minimized conformers. Analysis of the quality of the final structure was accomplished using PROCHECK-NMR and Aqua.[30] The following servers were used for the sequence and structural analyses: BLAST (http://blast.ncbi.nlm.nih.gov/Blast.cgi), DALI (http://ekhidna.biocenter.helsinki.fi/dali-server), and SCOP (http://scop.mrc-lmb.cam.ac.uk/scop).

NMR Chemical Shift Experiments. NMR chemical shift experiments with ^{15}N-labeled apo-HP1264 and unlabeled FMN/NADH were conducted on a Bruker AMX 500 spectrometer by acquiring the 2D $^{1}H-^{15}N$ HSQC spectra. Throughout the NMR titration experiments, the HP1264 concentration was maintained at 0.4 mM while the concentration of FMN/NADH was increased from 0 to 2 mM. All titration buffer conditions were maintained at 25 °C in 20 mM NaH_2PO_4/Na_2HPO_4 buffer (pH 6.0) containing 150 mM NaCl. Chemical shift perturbation analysis was performed by recording the chemical shift value of each peak before the titration and at ligand saturation. Average chemical shift perturbation values ($\Delta\delta_{avg}$) for ^{15}N and ^{1}H nuclei were derived as follows from eq 1:

$$\Delta\delta_{avg} = (0.2\Delta\delta_N{}^2 + \Delta\delta_H{}^2)^{1/2} \quad (1)$$

where $\Delta\delta_N$ and $\Delta\delta_H$ represent the chemical shift perturbation values of the amide nitrogen and proton, respectively. Chemical

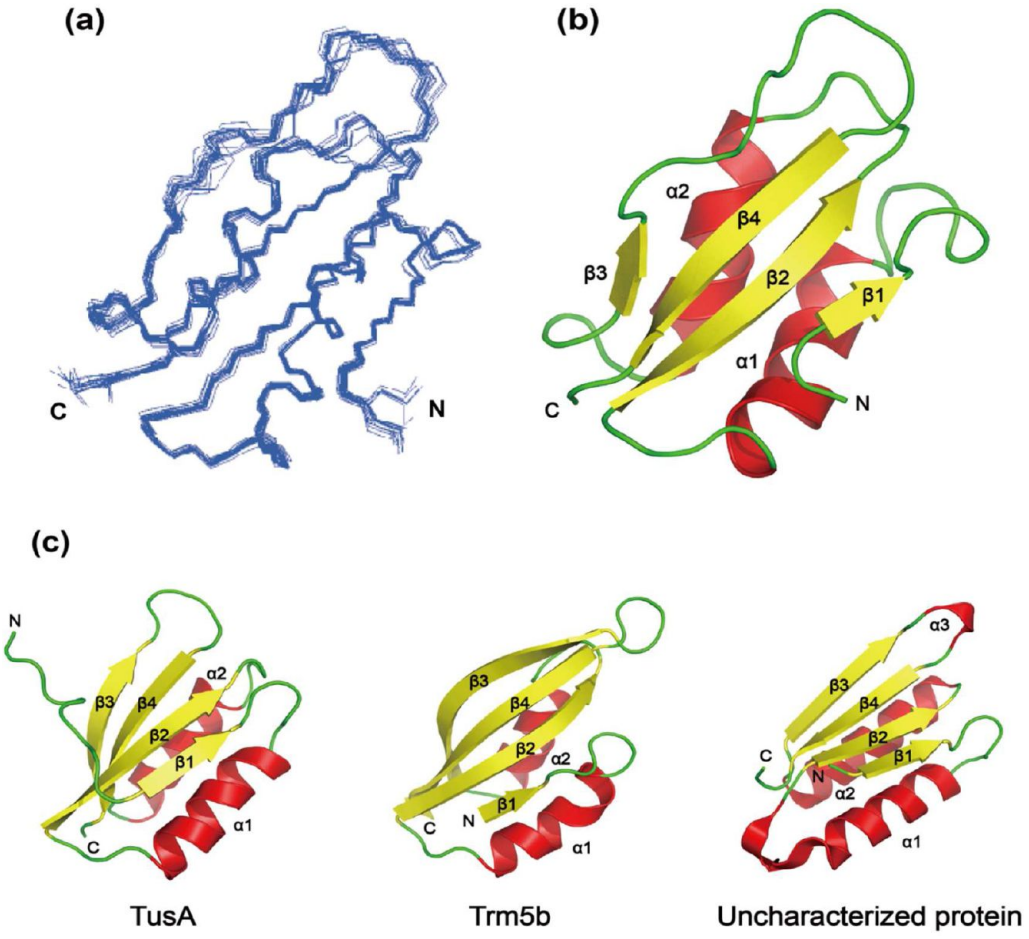

Figure 1. NMR structure of HP1264 and its structural homologues. (a) NMR structure of HP1264. The structure is represented as the backbone superposition of the 20 best energy-refined conformers. (b) Ribbon representation of the structure of HP1264. HP1264 shows a two-layer α/β-sandwich structure with a $\beta1\alpha1\beta2\alpha2\beta3\beta4$ topology. (c) Ribbon representation of structural homologues. The homologue structures with a DALI Z score of >8.0 are shown. The secondary structures of panels b and c are displayed as follows: red α-helices, yellow β-strands, and green loops.

shift perturbations were determined to be significant if they were >0.1 ppm for HP1264.

Calculation of K_d and Binding Stoichiometry. The NMR and fluorescence data were plotted as cumulative fluorescence or chemical shift changes versus the concentration of added HP1264 or FMN. The measured signals were subtracted from the signals of the reference buffer titrations. MATLAB was used to perform data fitting, and values for K_d were determined by using eq 2:

$$\Delta_{obs} = \Delta_{max}\left\{\left[K_d + S + N - \sqrt{(K_d + S + N)^2 - 4SN}\right] \Big/ 2N\right\} \quad (2)$$

where Δ_{obs} is the observed signal change at each titration point, Δ_{max} is the maximal observed signal change during the titration, K_d is the dissociation constant, S is the added substrate concentration, and N is the concentration of binding sites. In the formula, Δ_{obs} and Δ_{max} can be used for the NMR chemical shift or fluorescence changes. The first extrapolated line was generated by using a gradient of the start point of the plot. A formula for the gradient was derived by differentiating the equation. The second extrapolated line is generated as a maximal fluorescence change (Δ_{max}). The break point of two lines on the X-axis corresponds to the HP1264−FMN binding stoichiometry or the inverse form.

RESULTS AND DISCUSSION

HP1264 Is an Unusual Subunit of Complex I. On the basis of the arrangement of complex I structural genes,[31] *hp1264*, *hp1265*, and *hp1266* genes of *H. pylori* correspond to typical *nqo2*, *nqo1*, and *nqo3* genes of complex I, respectively, the products of which comprise the NADH dehydrogenase domain of complex I.[16] However, HP1264 and HP1265 share no significant sequence homology with the complex I subunits, including NQO2 and NQO1, from any other organisms except for *H. pylori* and *Campylobacter jejuni*.[32] This observation poses an important question about their functional and structural roles in complex I, given the possibility that both HP1264 and HP1265 lack the function of the NADH dehydrogenase domain. In general, this domain is involved in the binding to both FMN and NADH, and a coupled reduction−oxidation reaction between them triggers an electron transfer system of complex I.

Recently, it has been reported that uncharacterized reading frames (URFs) exist in a gene cluster of complex I from some organisms; for example, there are six URFs in *Paracoccus denitrificans*, seven in *Rhodobacter capsulatus*, and seven in *Neisseria meningitidis*.[31] Many of these genes encode proteins

dx.doi.org/10.1021/bi301714a | *Biochemistry* 2013, 52, 1583−1593

with no resemblance to typical complex I subunits and proteins of known function. Therefore, the functional roles of URFs in the complex I system remain to be established. However, it has been reported that some URFs encode proteins homologous to proteins of known function. For example, URF5 and URF6 of *P. denitrificans* encode proteins similar to the γ-carboxymuconolactone decarboxylase of *Acinetobacter calcoaceticus*, which produces β-ketoadipate enol lactone.[33] In *E. coli*, lactone can induce expression of the FMN-dependent NAD(P)H diaphorase.[33] On the basis of these facts, the URF5 and URF6 products could be hypothesized to be related to the regulation of complex I biosynthesis. This hypothesis might also be applied to unusual complex I genes, including *hp1264* and *hp1265* genes of *H. pylori*. However, it is noteworthy that these *H. pylori* genes are located in place of *nqo2* and *nqo1* genes, respectively, while URFs are commonly located between typical 14 genes in a gene cluster of complex I. On the basis of these observations, one could speculate that a defective *H. pylori* complex I would be created if the products of the *hp1264* and *hp1265* genes are less functional in complex I than those of *nqo2* and *nqo1* genes. However, it seems that the URF products are not necessarily required for the functional integrity of complex I because there are extra genes in the complex I operon.

HP1264 studied in this paper is a small protein composed of 76 amino acids with a molecular mass of ∼8.9 kDa and has no conserved cysteine residues that may coordinate the Fe−S center necessary for the relay of electrons across complex I. This feature is different from those of typical complex I subunits, allowing us to postulate that HP1264 could have unusual structural and biological roles in the complex I system. One possibility is that HP1264 bears novel binding motifs for NADH or FMN in the NADH dehydrogenase domain of complex I. Another possibility is that HP1264 provides a docking site for one or several substrates other than NADH, which are able to deliver electrons to Fe−S clusters of HP1265 or HP1266. It has been reported that *C. jejuni* complex I accepts electrons from flavodoxin rather than NADH.[34] In conclusion, diverse structural and functional possibilities have to be considered when studying HP1264, one of the unusual subunits of complex I from *H. pylori*.

Solution Structure of HP1264. To determine the solution structure of HP1264 by NMR spectroscopy, 2D NMR (^{1}H−^{15}N HSQC) spectra were first acquired to evaluate whether HP1264 is well-structured and to optimize sample conditions for additional 3D NMR measurements. The ^{1}H−^{15}N HSQC spectrum of ^{15}N-enriched HP1264 showed well-dispersed cross-peaks, indicating that the overall structure of HP1264 is well-defined. Conventional 3D NMR data were collected and used to assign most of the ^{1}H, ^{13}C, and ^{15}N resonances of the backbone and side chain atoms of HP1264. On the basis of the resonance assignments of HP1264, the final solution structure of HP1264 was determined by diverse restraints. The solution structure of HP1264 is represented as the backbone superposition of an ensemble of the 20 lowest-energy structures (Figure 1a). The structural statistics are summarized in Table 1. The 20 final structures are well-converged with a root-mean-square deviation (rmsd) of 0.46 Å for the backbone atoms and 0.83 Å for all heavy atoms. The structural quality could also be provided by the Ramachandran analysis of the ensemble that classifies the residues of HP1264 into the most favored (82.1%), additional allowed (16.1%), generously allowed (1.7%), and disallowed (0.1%) regions.

Table 1. Structural Statistics for the Final 20 Energy-Minimized Conformers of HP1264

no. of NOE upper distance constraints	
all	975
short-range ($\|i-j\| \leq 1$)	501
medium-range ($2 \leq \|i-j\| \leq 4$)	177
long-range ($\|i-j\| \geq 5$)	297
no. of dihedral angle constraints	
all	86
Φ	43
Ψ	43
no. of hydrogen bond constraints	21
rmsd from the average coordinate (Å)	
backbone atoms (N, Cα, CO)	0.46 ± 0.13
all heavy atoms	0.83 ± 0.13
deviation from idealized geometry	
bonds (Å)	0.000863 ± 0.000062
angles (deg)	0.254 ± 0.0021
CNS energy (kcal/mol)[a]	
$E_{overall}$	53.76 ± 0.72
E_{bond}	0.76 ± 0.078
E_{angle}	38.50 ± 0.34
$E_{improper}$	1.64 ± 0.15
E_{vdw}	12.25 ± 0.88
E_{noe}	0.56 ± 0.21
E_{cdih}	0.05 ± 0.02
Ramachandran plot (%)[b]	
most favored region	82.1
additionally allowed region	16.1
generously allowed region	1.7
disallowed region	0.1

[a]The default parameters and force constants of protein-allhydg5-4.param and anneal.inp in CNS 1.3 were used for structure calculation. [b]PROCHECK-NMR was used for calculation.

HP1264 folds into a compact two-layer α/β-sandwich structure with a β1α1β2α2β3β4 topology, comprising a mixed four-stranded β-sheet stacked against two α-helices, both of which are nearly parallel to the strands of the β-sheet (Figure 1b). The β-strands correspond to residues 3−5 (β1), 28−35 (β2), 55−57 (β3), and 68−74 (β4), while the α-helices correspond to residues 20−24 (α1) and 40−50 (α2). The secondary structures of HP1264 are packed and stabilized by forming an interior extensive hydrophobic core with 11 hydrophobic residues. On the basis of the SCOP database,[35] it is revealed that HP1264 adopts an IF3 (translation initiation factor 3)-like fold. In common, this fold has a core β1α1β2α2β3β4 topology with two layers and antiparallel strand 4.

Structural Comparisons of HP1264. The past decade has been marked by outstanding advances in understanding the structure of bacterial complex I at an atomic level.[16,18] In particular, the only determined structure of the hydrophilic domain of bacterial complex I was that from *T. thermophilus*. NQO2 is one of the eight subunits of this structure and might correspond to HP1264, which is also known as complex I subunit E from *H. pylori*. However, we found that HP1264 has a low degree of structural similarity to NQO2. In the SCOP database, NQO2 is divided into an N-terminal helical bundle and C-terminal thioredoxin fold. This fact supports the idea that HP1264 may play different structural and functional roles

dx.doi.org/10.1021/bi301714a | *Biochemistry* 2013, 52, 1583−1593

in the electron transfer mechanism of complex I compared to that of NQO2.

We searched for structural homologues of HP1264 within the Protein Data Bank (PDB)[36] by submitting the lowest energy-minimized NMR conformer of HP1264 to the fold recognition program DALI.[37] The results showed that structural homologues with a DALI Z score of >7.0 are sulfurtransferase TusA from *E. coli* (PDB entry 1dcj, Z score = 9.4 for the NMR structure, and rmsd = 2.0), the C-terminal domain of tRNA-methyltransferase Trm5b from *Methanocaldococcus jannaschii* (PDB entry 3ay0, Z score = 8.3, and rmsd = 2.3), an uncharacterized protein from *Desulfitobacterium hafniense* (PDB entry 3hz7, Z score = 8.0, and rmsd = 2.6), and the C-terminal domain of ribosomal protein L11 methyltransferase from *T. thermophilus* (PDB entry 3cjt, Z score = 7.3, and rmsd = 2.2). The structures of three proteins with a Z score of >8.0 are shown in Figure 1c. In particular, sulfurtransferase TusA is structurally most similar to HP1264, although the level of sequence identity between them is as low as ∼15.9%. In the SCOP database, sulfurtransferase TusA adopts an IF3-like fold and belongs to the SirA-like superfamily implicated in cell division.[38,39] We found that the structural motifs involved in the activities of the structural homologues are not conserved in HP1264.[40,41] Therefore, it was difficult to deduce a biological function of HP1264 by looking into the functions of the structural homologues.

HP1264 Interacts with FMN. FMN-free HP1264 was obtained using the method presented in Materials and Methods and confirmed by its characteristic UV−visible spectrum showing a single absorption maximum at 279 nm (data not shown). Subsequently, we assessed the binding of FMN to HP1264 by UV−visible spectroscopy. Absorption peak changes of FMN in UV−visible spectra could be a strong indication that FMN is bound to a flavoprotein. As shown in Figure 2, free FMN exhibits absorption maxima at 373 and 445 nm, and the addition of HP1264 to FMN caused a perturbation of these maxima. The spectral changes show a hypsochromic shift of the absorption peak from 373 to 364 nm and a bathochromic shift of the absorption peak from 445 to 456 nm. Both shifts are accompanied by a reduction in the intensity. These results suggest that the UV−visible absorption of FMN could be influenced by the binding of HP1264.

On the basis of the fact that FMN and NADH have respective fluorogenic moieties such as an isoalloxazine ring and nicotinamide, fluorescence quenching experiments are useful for investigating whether FMN or NADH binds to HP1264.[42] Their intrinsic fluorescences would be quenched if they were bound to HP1264. In general, these phenomena are concomitant with the changes in the local electronic environments around the fluorogenic moieties. As shown in Figure 3a, the quenching of FMN fluorescence upon the addition of HP1264 was monitored at wavelengths ranging from 450 to 660 nm, and we obtained the fluorescence emission spectra of FMN in the presence of increasing amounts of HP1264. As a

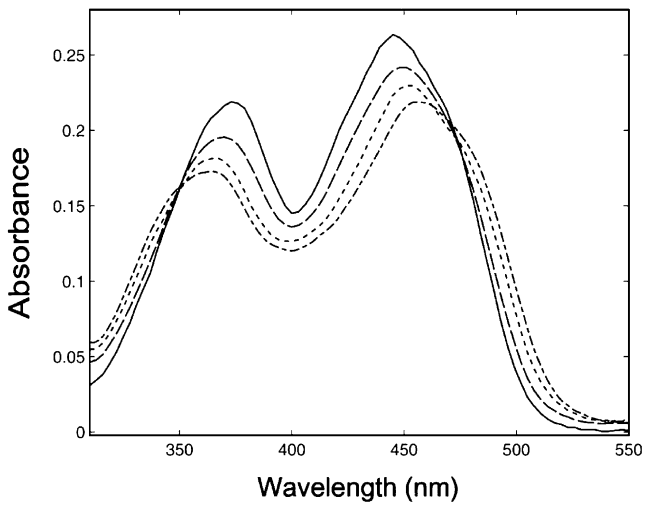

Figure 2. Spectrophotometric titration of FMN with HP1264. Absorption spectra of 20 μM FMN were recorded in the presence of 0 (—), 40 (– – –), 80 (---), and 120 μM HP1264 (-·-·-). All spectra were recorded at 25 °C in 20 mM NaH_2PO_4/Na_2HPO_4 buffer (pH 6.0) and 150 mM NaCl.

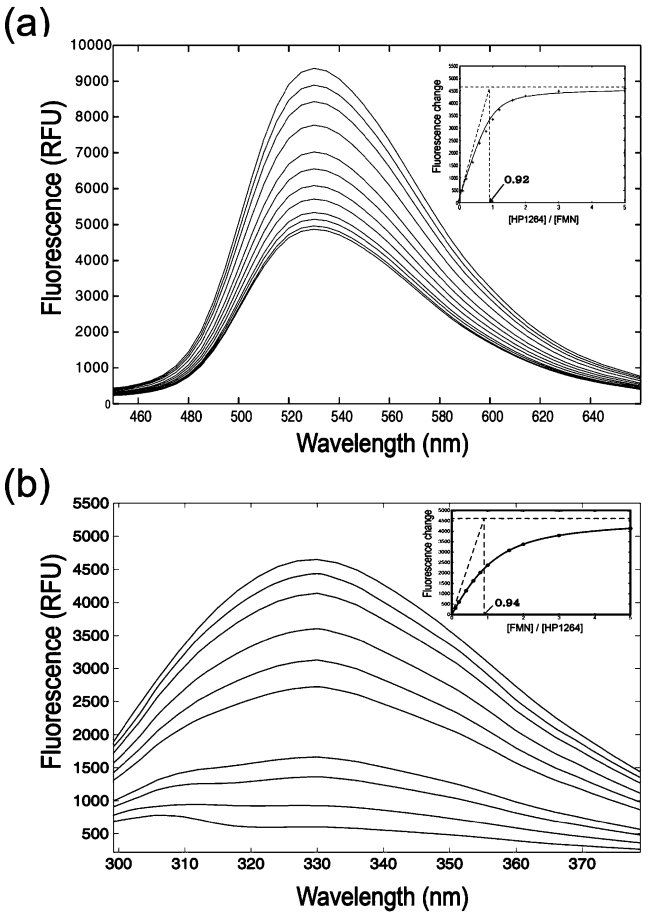

Figure 3. Fluorescence quenching of FMN and HP1264. (a) FMN fluorescence quenching upon HP1264 binding. Fluorescence spectra of 0.4 mM FMN were recorded in the absence and presence of HP1264. From top to bottom, the protein concentrations were 0, 0.04, 0.08, 0.16, 0.24, 0.32, 0.4, 0.48, 0.64, 0.8, 1.2, and 2.0 mM, respectively. In the inset, the fluorescence changes at 528 nm are plotted against the HP1264:FMN molar ratio. The arrow indicates the HP1264−FMN binding stoichiometry. (b) HP1264 fluorescence quenching upon FMN binding. Fluorescence spectra of 100 μM HP1264 were recorded in the absence and presence of FMN. From top to bottom, FMN concentrations were 10, 20, 40, 60, 80, 100, 160, 200, 300, and 500 μM, respectively. In the inset, the fluorescence changes at 330 nm are plotted against the FMN:HP1264 molar ratio. The arrow indicates the FMN−HP1264 binding stoichiometry. All spectra in panels a and b were recorded at 25 °C in 20 mM NaH_2PO_4/Na_2HPO_4 buffer (pH 6.0) and 150 mM NaCl.

dx.doi.org/10.1021/bi301714a | *Biochemistry* 2013, 52, 1583−1593

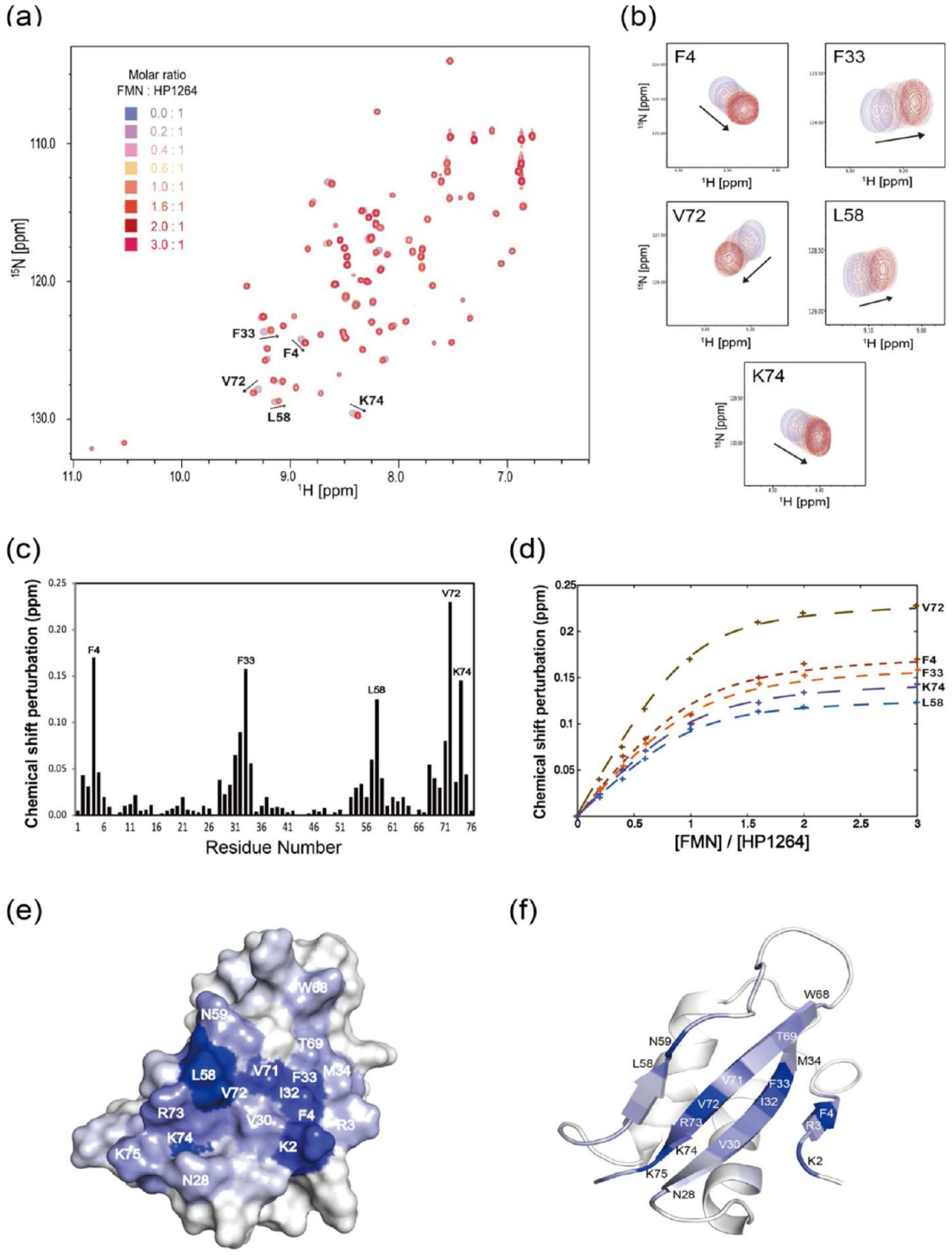

Figure 4. NMR-based titration of ^{15}N-labeled HP1264 with FMN. (a) Overlay of the ^{15}N−^{1}H HSQC spectra of HP1264 with increasing amounts of added FMN. ^{15}N−^{1}H HSQC spectra of HP1264 (0.4 mM) were recorded in the absence of FMN and in the presence of 0.04, 0.08, 0.16, 0.24, 0.4, 0.64, 0.8, and 1.2 mM FMN. The titration spectra are all color-coded according to the FMN:HP1264 molar ratio. (b) Expanded views of the ^{15}N−^{1}H HSQC spectra. The signal changes for residues F4, F33, L58, V72, and K74 are shown as representatives of the significant chemical shift changes for HP1264. (c) Graph of the amide chemical shift perturbations with respect to the residues of HP1264. Residues F4, F33, L58, V72, and K74 with chemical shift perturbations of >0.1 ppm are indicated. (d) NMR titration curves for residues F4, F33, L58, V72, and K74. The chemical shift perturbation values are plotted as a function of the FMN:HP1264 molar ratio. (e) Chemical shift mapping onto a surface representation of HP1264. Residues are colored according to a gradient derived from their chemical shift perturbation value, such that a darker blue represents a larger perturbation. (f) Chemical shift mapping onto a ribbon representation of HP1264. The residues showing large chemical shift changes are most distributed in the β-sheet of HP1264. The labeled residues and color coding are the same as in panel e.

result, the level of quenching of FMN fluorescence increased as the concentration of added HP1264 increased, indicating that HP1264 can bind to FMN. We also observed that the addition of a 5-fold molar excess of HP1264 (2 mM) over the amount of

dx.doi.org/10.1021/bi301714a | *Biochemistry* 2013, 52, 1583−1593

FMN (0.4 mM) leads to binding saturation. At the emission wavelength of 528 nm showing the highest FMN fluorescence in this experiment, the maximal quenching of FMN fluorescence was estimated to be ~52% when FMN was bound to HP1264.

The FMN fluorescence signals at a wavelength of 528 nm were subtracted by the reference titration signals that were measured only in the presence of FMN, and the differences (termed fluorescence quenching) were plotted against the increasing concentration of HP1264 added (Figure 3a, inset). The data were fit to a single-site binding model, using a least-squares fitting search to derive the best value of K_d from the standard binding equation (eq 2, Materials and Methods). The calculated K_d value was 54 ± 10 μM (95% confidence interval), showing a relatively weak binding affinity among the flavoproteins. In addition, the extrapolated break point for the maximal fluorescence change corresponds to the binding of an ~0.92 molar ratio of HP1264 to FMN (Figure 3a, inset). Given the possibility that a fraction of the purified protein may be inactive or that the exact measurement of the protein concentration may be difficult, we concluded that there is one FMN binding site per HP1264 monomer.

In the case of the NADH titration with HP1264, NADH fluorescence upon addition of HP1264 was recorded at wavelengths ranging from 400 to 620 nm. However, no significant quenching of NADH fluorescence was detected, although a >10-fold molar excess of HP1264 over NADH was used, indicating that HP1264 cannot bind to NADH (data not shown). A similar titration of NADH with FMN-bound HP1264 was performed, but a positive signal for the interaction between them was not observed (data not shown). These results are consistent with the previous hypothesis that complex I of *H. pylori* could accept electrons from a substrate rather than NADH. It is also possible to formulate a new hypothesis that HP1265 or HP1266 could have a novel NADH binding motif because they are thought to be adjacent to HP1264 in the NADH dehydrogenase domain.

In conclusion, HP1264 was identified as a novel FMN binding protein. This result was corroborated by the following data from tryptophan fluorescence and NMR experiments. This finding suggests the biological implication that FMN-bound HP1264 could participate in the beginning of the electron transfer pathway of complex I from *H. pylori*. However, in *T. thermophilus* complex I, both FMN and NADH can bind to the NQO1 subunit, which might correspond to complex I subunit F (HP1265) from *H. pylori*.[16,32] The FMN binding subunits of complex I are different between *H. pylori* and *T. thermophilus*, implying that the initial electron transfer mechanisms of complex I might also be different between them.

HP1264 Tryptophan Is Important for FMN Binding. On the basis of the fact that HP1264 has one tryptophan residue (Trp68) that is relatively exposed to a solvent, we performed fluorescence titration of HP1264 with FMN to explore whether HP1264 tryptophan is involved in FMN binding. The tryptophan fluorescence would be quenched if this residue interacts with FMN. Figure 3b shows fluorescence emission spectra for HP1264 bound to FMN. The fluorescence in the presence of increasing amounts of FMN was monitored at wavelengths ranging from 300 to 380 nm. As a result, the addition of FMN led to a decrease in the fluorescence intensity of HP1264 at the emission maximum (330 nm) without its notable shift. We also observed that the addition of a 5-fold molar excess of FMN (0.5 mM) over HP1264 (0.1 mM) completely quenched the tryptophan fluorescence. These results indicated that HP1264 tryptophan is important for FMN binding.

Using the previous method for processing the FMN fluorescence spectra, the degrees of fluorescence quenching of HP1264 were plotted versus the FMN:HP1264 molar ratio (Figure 3b, inset), and a K_d value for the interaction between HP1264 and FMN was calculated to be 46 ± 5 μM (95% confidence interval). In addition, the extrapolated break point for the maximal fluorescence change corresponds to the binding of an ~0.94 molar ratio of FMN to HP1264, implying that one FMN binding site exists in HP1264.

FMN Binding Site of HP1264. We conducted NMR chemical shift experiments with ^{15}N-labeled HP1264 upon binding to FMN or NADH using 2D (^{1}H−^{15}N HSQC) NMR spectroscopy. This method is useful for gaining residue-specific information about the HP1264−ligand interaction or conformational changes of HP1264 upon ligand binding. We compared the ^{1}H−^{15}N HSQC spectra acquired from the ^{15}N-labeled HP1264 (the observed partner) alone and with increasing concentrations of unlabeled FMN (the unobserved partner). These comparable spectra are shown as an overlay in Figure 4a. The peak movements without line broadening in the spectra indicate that the HP1264−FMN interaction is dynamically in a fast exchange regime. In addition, the peaks showing chemical shift changes during the titration correspond to amino acid residues that experience changes in local chemical environments caused by the HP1264−FMN interaction. However, large chemical shift changes for only some residues were observed, suggesting that, upon FMN binding, HP1264 shows no significant overall conformational changes. A similar NMR titration of NADH to ^{15}N-labeled HP1264 was performed; however, no chemical shift changes for HP1264 were induced by the addition of NADH, implying a lack of interaction between HP1264 and NADH (data not shown). This result was consistent with the previous NADH fluorescence data.

On the basis of the assigned backbone ^{1}H and ^{15}N resonances of HP1264, the values of the chemical shift changes for each residue could be calculated from the simple chemical shift perturbation equation (eq 1, Materials and Methods). We were able to observe significant chemical shift changes for specific residues, such as Phe4, Phe33, Leu58, Val72, and Lys74, when FMN bound to HP1264 (Figure 4b). To investigate the FMN binding property of HP1264, we constructed the NMR titration curves for these five residues (Figure 4d). Using the same method that was used to process the fluorescence titration curves, we determined a binding stoichiometry ratio of ~0.95:1 (HP1264:FMN) and an average K_d of 60 ± 12 μM (95% confidence interval) for the interaction between HP1264 and FMN. The values of the binding parameters are highly similar to those derived from the previous fluorescence experiments.

Furthermore, we characterized a potential FMN binding region of HP1264 by following the shifted peaks in the ^{1}H−^{15}N HSQC spectra. To quantitatively treat the peak movements at binding saturation, we generated chemical shift perturbation values for the peaks by comparing the spectra of the ^{15}N-labeled HP1264 alone and with a 3-fold molar excess of FMN over HP1264. These values are plotted with respect to the residues of HP1264 (Figure 4c). As a result, the residues showing relatively high values (>0.05 ppm) are most distributed in the β-sheet of HP1264, indicating that this

dx.doi.org/10.1021/bi301714a | *Biochemistry* 2013, 52, 1583−1593

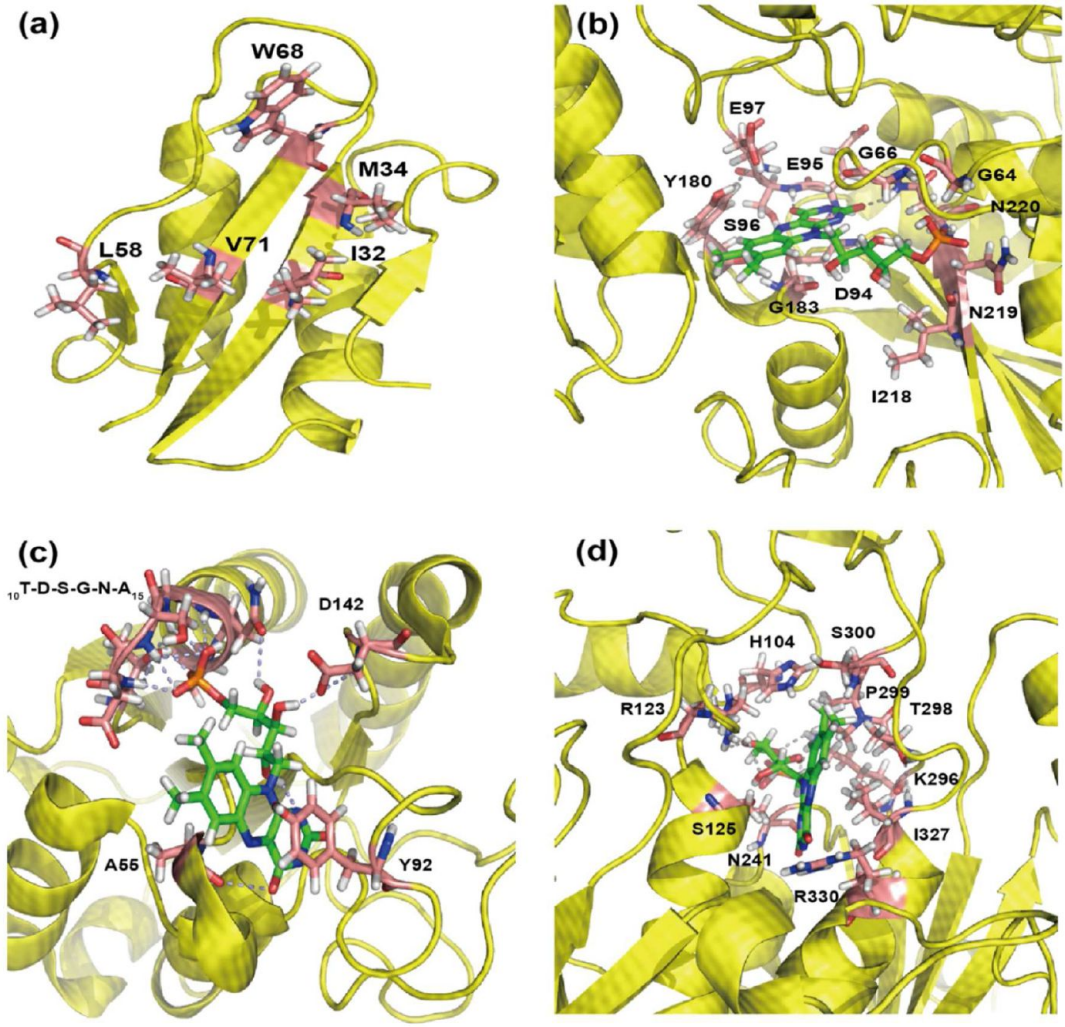

Figure 5. Structural comparisons of FMN binding sites. (a) Potential FMN binding site of HP1264. The candidate residues for FMN binding are indicated. (b) FMN binding site of NQO1 from *T. thermophilus*. (c) FMN binding site of the flavodoxin from *H. pylori*. (d) FMN binding site of the chorismate synthase from *H. pylori*. Overall structures in all figures are represented as ribbon models. FMN and the residues covering the FMN binding sites are shown as sticks with hydrogen bonds shown as gray dotted lines. Nitrogen, oxygen, hydrogen, and phosphorus atoms are colored blue, red, white, and orange, respectively. Carbon atoms of the residue side chain and FMN are colored light pink and green, respectively.

region could be involved in FMN binding. The mapping of chemical shift perturbations onto the surface and ribbon representations of HP1264 is shown in panels e and f of Figure 4, respectively. Because HP1264 has no deep cavity for comfortable FMN binding, it seems likely that the binding affinity between them is relatively weak and that the surface-exposed β-sheet region could efficiently accommodate FMN, but not the more bulky NADH.

We developed the idea that the β-sheet of HP1264 is important for FMN binding. The NMR chemical shift data were not sufficient to explain the FMN binding site in full detail. Despite the limitation of the NMR data, we predicted candidate residues of HP1264 for FMN binding by establishing three reasonable criteria. First, FMN binding residues should exhibit chemical shift changes of >0.05 ppm. This criterion is based on the previous fluorescence data that showed that residue Trp68 is involved in FMN binding. The backbone NH peak of this residue showed a chemical shift perturbation value of ~0.05 ppm when FMN bound to HP1264. Following the first criterion, we selected the 10 possible residues for FMN binding, which are Phe4, Ala31, Ile32, Phe33, Met34, Leu57, Leu58, Val71, Val72, and Lys74. Second, the FMN binding site should be spatially close to residues Phe4, Phe33, Leu58, Val72, and Lys74. These five residues show the significant chemical changes (>0.1 ppm). Therefore, it is rational to assume that these residues and the region around them are involved in FMN binding. Among the 10 residues satisfying the first criterion that are listed above, nine residues, Phe4, Ile32, Phe33, Met34, Leu57, Leu58, Val71, Val72, and Lys74, satisfy the second criterion. Third, the side chains of FMN binding residues should be surface-exposed because the side chains buried in the interior of the protein might have difficulty in interacting directly with FMN. Among the nine residues satisfying the first and second criteria listed above, four residues, Ile32, Met34, Leu58, and Val71, satisfy the third criterion. Taken together, we propose that in addition to Trp68, residues Ile32, Met34, Leu58, and Val71 of the β-strands could be candidate residues for the contact with FMN (Figure 5a). Furthermore, it is conceivable that these proposed residues could bind to the isoalloxazine ring of FMN by hydrophobic interactions. However, structural details of the

dx.doi.org/10.1021/bi301714a | *Biochemistry* 2013, 52, 1583−1593

interaction between HP1264 and FMN remain to be elucidated.

Association of FMN with Neighboring Subunits of HP1264. We present the first evidence that HP1264 can bind to FMN but not to NADH. However, it remains unclear whether HP1264 binds more tightly to FMN by assistance from its neighboring subunits in complex I. On the basis of the subunit arrangement of complex I in *T. thermophilus*, HP1265 (37.2 kDa) and HP1266 (94.2 kDa) are predicted to be located in the vicinity of HP1264.[16,32] It is possible that two or all three of these subunits could be cooperatively involved in the binding to FMN, in which case the FMN binding site of complex I should be shared with HP1264 and its nearby subunit. This possibility could be supported by our previous result that the binding affinity between HP1264 and FMN is low. It could also be suggested that transient binding of FMN to HP1264 is needed prior to attaining the final catalytic structure of complex I. In this case, one or more of the neighboring subunits of HP1264 should have a higher affinity for FMN than HP1264, facilitating the transfer of FMN from HP1264 to its neighboring subunit. On the other hand, HP1264 could be conceived to serve as a primary subunit for FMN binding and thus to act as an independently FMN-related subunit. This assumption could be supported by the fact that some flavoproteins can exert their biological activities in spite of their weak FMN binding: for example, *E. coli* WrbA displays NAD(P)H:quinone oxidoreductase activity, although it has a low affinity for FMN with a K_d in the micromolar range.[43,44]

In general, an initial electron transfer within complex I is achieved between its internal redox centers such as FMN and the Fe−S cluster, both of which must be close to each other. In *T. thermophilus* complex I, electrons could be transferred between FMN and the Fe−S cluster in the same NQO1.[16] The presence of the FMN binding pocket in NQO1 could facilitate this electron transfer process, possibly because FMN bound in the pocket could be more accessible to the Fe−S cluster. In contrast to NQO1, HP1264 has only one redox center, FMN, suggesting that reduced FMN should donate electrons to the Fe−S cluster in a neighboring subunit of HP1264. In this case, it would be unsuitable that HP1264 adopts an FMN binding pocket, because the intersubunit distance between FMN and the Fe−S cluster is large enough that electrons are not transferred between them. This assumption is consistent with our finding that HP1264 has the surface-exposed region for FMN binding. However, an energetically stable FMN binding would be inevitably sacrificed in this surface binding mode, accompanied by a low affinity between HP1264 and FMN.

Novel Site and Fold for FMN Binding. It has recently been reported that a variety of FMN binding protein folds are widely distributed throughout all kingdoms of life. Because HP1264 was thought to be the complex I subunit capable of FMN binding, the structure of HP1264 was preferentially compared with the previously determined structure of the NQO1 subunit of complex I from *T. thermophilus*,[16] which can bind to FMN. Notably, the Rossmann fold-like domain of NQO1 has a frequently occurring motif that binds to nucleotides such as FMN, FAD, NADH, etc.[45] In the SCOP database, this domain of NQO1 is classified as a NQO1 FMN binding domain-like fold (Table 1 of the Supporting Information). However, little structural similarity was observed between the IF3-like fold of HP1264 and the NQO1 FMN binding domain-like fold. Therefore, it is conceivable that HP1264 has structurally evolved in a different manner to have a new fold with the FMN binding function when compared to NQO1. The FMN binding of NQO1 is mostly achieved by a hydrogen bond network at the end of a solvent-exposed cavity.[16] Figure 5b shows that various residues of NQO1 are involved in FMN binding at the cavity. FMN interacts mainly with the $\alpha3-\alpha4$ loop (Gly64 and Gly66), the $\beta1-\alpha5$ loop (Asp94, Glu95, Ser96, and Glu97), $\alpha8$ (Tyr180 and Gly183), and $\beta4$ (Ile218, Asn219, and Asn220), suggesting that the FMN binding mechanism of NQO1 is different from that of HP1264.

In the SCOP database, FMN binding folds from *H. pylori* have recently been classified into a flavodoxin-like fold and chorismate synthase fold, respectively (Table 1 of the Supporting Information). The flavodoxin-like fold from *H. pylori* can bind to the phosphoribityl tail of FMN by hydrogen bonds and to the isoalloxazine ring of FMN by hydrophobic interactions (Figure 5c).[46] The phosphate group of FMN is bound by the loop motif (Thr-Asp-Ser-Gly-Asn-Ala), and the ribityl part of FMN is bound by the side chain atoms of Asn14 and Asp142. The isoalloxazine ring is bound by residues Tyr92 and Ala55 at the *si*-face and the *re*-face of the isoalloxazine ring, respectively. The chorismate synthase fold from *H. pylori* exhibits a highly positive electrostatic potential at the surface of the FMN binding pocket.[47] Diverse regions, including $\alpha2$ (His104), the $\alpha2-\alpha3$ loop (Arg123), $\alpha3$ (Ser125), $\beta11$ (Asn241), $\beta16$ (Lys296), the $\beta16-\beta17$ loop (Thr298, Pro299, and Ser300), and $\alpha8$ (Ile327 and Arg330), contribute to the formation of this FMN binding pocket (Figure 5d). This bioinformatics study revealed that the previously known FMN binding sites and folds from *H. pylori* were not conserved in HP1264.

Furthermore, we found that the IF3-like fold and the proposed FMN binding site of HP1264 are not similar to those of any other FMN binding proteins described so far in the literature or in the bioinformatics database. A systematic study of the SCOP database revealed that 14 protein folds in complex with FMN are structurally determined (Table 1 of the Supporting Information). These folds show distinctive features according to the spatial arrangements of the secondary structure elements. The HP1264 fold presented here could be classified into the 15th protein fold for FMN binding. However, it remains unclear whether HP1264 and its neighboring subunits cooperatively form a FMN binding fold of complex I. Further study is necessary to determine the overall structure and exact FMN binding mode of complex I from *H. pylori*.

■ ASSOCIATED CONTENT

Supporting Information

Diverse FMN binding folds in the SCOP database. This material is available free of charge via the Internet at http://pubs.acs.org.

Accession Codes

The coordinates of the HP1264 structure reported in this paper are deposited in the PDB as entry 2LXR.

■ AUTHOR INFORMATION

Corresponding Author

*E-mail: lbj@nmr.snu.ac.kr. Telephone: +82 2 880 7869. Fax: +82 2 872 3632.

Present Address

[†]Center for Structural Biology and Departments of Biochemistry and Pharmacology, Vanderbilt University School of Medicine, Nashville, TN 37232-8725.

Funding

This study was supported by a National Research Foundation of Korea (NRF) grant funded by the Korean government (MEST) (2012R1A2A1A01003569 and 20110001207). This study was also supported by a grant from the Korea Healthcare technology R&D Project, Ministry for Health, Welfare & Family Affairs, Republic of Korea (A092006). This work was supported in part by the 2012 BK21 project for Medicine, Dentistry, and Pharmacy.

Notes

The authors declare no competing financial interest.

■ ACKNOWLEDGMENTS

We thank the National Center for Inter-University Research Facilities (NCIRF) for use of their NMR machines.

■ ABBREVIATIONS

NADH, nicotinamide adenine dinucleotide; FMN, flavin mononucleotide; NMR, nuclear magnetic resonance; TusA, tRNA 2-thiouridine synthesizing protein A; SirA, sporulation inhibitor of replication protein A; IF3, translation initiation factor 3; SCOP, structural classification of proteins; NQO, NAD(P)H:quinone oxidoreductase; HSQC, heteronuclear single-quantum coherence; CYANA, combined assignment and dynamics algorithm; CSI, chemical shift index; BLAST, basic local alignment search tool.

■ REFERENCES

(1) Cover, T. L., and Blaser, M. J. (1996) *Helicobacter pylori* infection, a paradigm for chronic mucosal inflammation: Pathogenesis and implications for eradication and prevention. *Adv. Intern. Med. 41*, 85−117.

(2) Forman, D., Newell, D. G., Fullerton, F., Yarnell, J. W., Stacey, A. R., Wald, N., and Sitas, F. (1991) Association between infection with *Helicobacter pylori* and risk of gastric cancer: Evidence from a prospective investigation. *BMJ [Br. Med. J.] 302*, 1302−1305.

(3) Peek, R. M., Jr., and Blaser, M. J. (2002) *Helicobacter pylori* and gastrointestinal tract adenocarcinomas. *Nat. Rev. Cancer 2*, 28−37.

(4) Selgrad, M., Kandulski, A., and Malfertheiner, P. (2009) *Helicobacter pylori*: Diagnosis and treatment. *Curr. Opin. Gastroenterol. 25*, 549−556.

(5) Lochmannova, J. (2010) [Current perspective of the resistance of *Helicobacter pylori* strains to antimicrobial drugs]. *Klinická mikrobiologie a infekc□ní lékar□ství 16*, 199−202.

(6) Salama, N. R., Shepherd, B., and Falkow, S. (2004) Global transposon mutagenesis and essential gene analysis of *Helicobacter pylori*. *J. Bacteriol. 186*, 7926−7935.

(7) Galkin, A. S., Grivennikova, V. G., and Vinogradov, A. D. (1999) $\rightarrow H^+/2e^-$ stoichiometry in NADH-quinone reductase reactions catalyzed by bovine heart submitochondrial particles. *FEBS Lett. 451*, 157−161.

(8) Galkin, A., Drose, S., and Brandt, U. (2006) The proton pumping stoichiometry of purified mitochondrial complex I reconstituted into proteoliposomes. *Biochim. Biophys. Acta 1757*, 1575−1581.

(9) Walker, J. E. (1992) The NADH:ubiquinone oxidoreductase (complex I) of respiratory chains. *Q. Rev. Biophys. 25*, 253−324.

(10) Yagi, T., and Matsuno-Yagi, A. (2003) The proton-translocating NADH-quinone oxidoreductase in the respiratory chain: The secret unlocked. *Biochemistry 42*, 2266−2274.

(11) Brandt, U. (2006) Energy converting NADH:quinone oxidoreductase (complex I). *Annu. Rev. Biochem. 75*, 69−92.

(12) Sazanov, L. A. (2007) Respiratory complex I: Mechanistic and structural insights provided by the crystal structure of the hydrophilic domain. *Biochemistry 46*, 2275−2288.

(13) Dawson, T. M., and Dawson, V. L. (2003) Molecular pathways of neurodegeneration in Parkinson's disease. *Science 302*, 819−822.

(14) Balaban, R. S., Nemoto, S., and Finkel, T. (2005) Mitochondria, oxidants, and aging. *Cell 120*, 483−495.

(15) Carroll, J., Fearnley, I. M., Skehel, J. M., Shannon, R. J., Hirst, J., and Walker, J. E. (2006) Bovine complex I is a complex of 45 different subunits. *J. Biol. Chem. 281*, 32724−32727.

(16) Sazanov, L. A., and Hinchliffe, P. (2006) Structure of the hydrophilic domain of respiratory complex I from *Thermus thermophilus*. *Science 311*, 1430−1436.

(17) Efremov, R. G., Baradaran, R., and Sazanov, L. A. (2010) The architecture of respiratory complex I. *Nature 465*, 441−445.

(18) Efremov, R. G., and Sazanov, L. A. (2011) Structure of the membrane domain of respiratory complex I. *Nature 476*, 414−420.

(19) Bottcher, B., Scheide, D., Hesterberg, M., Nagel-Steger, L., and Friedrich, T. (2002) A novel, enzymatically active conformation of the *Escherichia coli* NADH:ubiquinone oxidoreductase (complex I). *J. Biol. Chem. 277*, 17970−17977.

(20) Guenebaut, V., Schlitt, A., Weiss, H., Leonard, K., and Friedrich, T. (1998) Consistent structure between bacterial and mitochondrial NADH:ubiquinone oxidoreductase (complex I). *J. Mol. Biol. 276*, 105−112.

(21) Berrisford, J. M., and Sazanov, L. A. (2009) Structural basis for the mechanism of respiratory complex I. *J. Biol. Chem. 284*, 29773−29783.

(22) Kudin, A. P., Bimpong-Buta, N. Y., Vielhaber, S., Elger, C. E., and Kunz, W. S. (2004) Characterization of superoxide-producing sites in isolated brain mitochondria. *J. Biol. Chem. 279*, 4127−4135.

(23) Macheroux, P. (1999) UV-Visible Spectroscopy as a Tool to Study Flavoproteins. In *Flavoprotein Protocols* (Chapman, S., and Reid, G., Eds.) pp 1−7, Humana Press, Totowa, NJ.

(24) Delaglio, F., Grzesiek, S., Vuister, G. W., Zhu, G., Pfeifer, J., and Bax, A. (1995) NMRPipe: A multidimensional spectral processing system based on UNIX pipes. *J. Biomol. NMR 6*, 277−293.

(25) Johnson, B. A., and Blevins, R. A. (1994) NMR View: A computer program for the visualization and analysis of NMR data. *J. Biomol. NMR 4*, 603−614.

(26) Guntert, P. (2004) Automated NMR structure calculation with CYANA. *Methods Mol. Biol. 278*, 353−378.

(27) Shen, Y., Delaglio, F., Cornilescu, G., and Bax, A. (2009) TALOS+: A hybrid method for predicting protein backbone torsion angles from NMR chemical shifts. *J. Biomol. NMR 44*, 213−223.

(28) Wishart, D. S., and Sykes, B. D. (1994) The ^{13}C chemical-shift index: A simple method for the identification of protein secondary structure using ^{13}C chemical-shift data. *J. Biomol. NMR 4*, 171−180.

(29) Brunger, A. T., Adams, P. D., Clore, G. M., DeLano, W. L., Gros, P., Grosse-Kunstleve, R. W., Jiang, J. S., Kuszewski, J., Nilges, M., Pannu, N. S., Read, R. J., Rice, L. M., Simonson, T., and Warren, G. L. (1998) Crystallography & NMR system: A new software suite for macromolecular structure determination. *Acta Crystallogr. D54*, 905−921.

(30) Laskowski, R. A., Rullmannn, J. A., MacArthur, M. W., Kaptein, R., and Thornton, J. M. (1996) AQUA and PROCHECK-NMR: Programs for checking the quality of protein structures solved by NMR. *J. Biomol. NMR 8*, 477−486.

(31) Smith, M. A., Finel, M., Korolik, V., and Mendz, G. L. (2000) Characteristics of the aerobic respiratory chains of the microaerophiles *Campylobacter jejuni* and *Helicobacter pylori*. *Arch. Microbiol. 174*, 1−10.

(32) Finel, M. (1998) Does NADH play a central role in energy metabolism in *Helicobacter pylori*? *Trends Biochem. Sci. 23*, 412−413.

(33) Xu, X., Matsuno-Yagi, A., and Yagi, T. (1993) DNA sequencing of the seven remaining structural genes of the gene cluster encoding the energy-transducing NADH-quinone oxidoreductase of *Paracoccus denitrificans*. *Biochemistry 32*, 968−981.

(34) Weerakoon, D. R., and Olson, J. W. (2008) The *Campylobacter jejuni* NADH:ubiquinone oxidoreductase (complex I) utilizes flavodoxin rather than NADH. *J. Bacteriol. 190*, 915−925.
(35) Andreeva, A., Howorth, D., Chandonia, J. M., Brenner, S. E., Hubbard, T. J., Chothia, C., and Murzin, A. G. (2008) Data growth and its impact on the SCOP database: New developments. *Nucleic Acids Res. 36*, D419−D425.
(36) Berman, H. M., Battistuz, T., Bhat, T. N., Bluhm, W. F., Bourne, P. E., Burkhardt, K., Feng, Z., Gilliland, G. L., Iype, L., Jain, S., Fagan, P., Marvin, J., Padilla, D., Ravichandran, V., Schneider, B., Thanki, N., Weissig, H., Westbrook, J. D., and Zardecki, C. (2002) The Protein Data Bank. *Acta Crystallogr. D58*, 899−907.
(37) Dietmann, S., Park, J., Notredame, C., Heger, A., Lappe, M., and Holm, L. (2001) A fully automatic evolutionary classification of protein folds: Dali Domain Dictionary version 3. *Nucleic Acids Res. 29*, 55−57.
(38) Katoh, E., Hatta, T., Shindo, H., Ishii, Y., Yamada, H., Mizuno, T., and Yamazaki, T. (2000) High precision NMR structure of YhhP, a novel *Escherichia coli* protein implicated in cell division. *J. Mol. Biol. 304*, 219−229.
(39) Ishii, Y., Yamada, H., Yamashino, T., Ohashi, K., Katoh, E., Shindo, H., Yamazaki, T., and Mizuno, T. (2000) Deletion of the yhhP gene results in filamentous cell morphology in *Escherichia coli*. *Biosci., Biotechnol., Biochem. 64*, 799−807.
(40) Ikeuchi, Y., Shigi, N., Kato, J., Nishimura, A., and Suzuki, T. (2006) Mechanistic insights into sulfur relay by multiple sulfur mediators involved in thiouridine biosynthesis at tRNA wobble positions. *Mol. Cell 21*, 97−108.
(41) Christian, T., Evilia, C., and Hou, Y. M. (2006) Catalysis by the second class of tRNA(m1G37) methyl transferase requires a conserved proline. *Biochemistry 45*, 7463−7473.
(42) Duurkens, R. H., Tol, M. B., Geertsma, E. R., Permentier, H. P., and Slotboom, D. J. (2007) Flavin binding to the high affinity riboflavin transporter RibU. *J. Biol. Chem. 282*, 10380−10386.
(43) Patridge, E. V., and Ferry, J. G. (2006) WrbA from *Escherichia coli* and *Archaeoglobus fulgidus* is an NAD(P)H:quinone oxidoreductase. *J. Bacteriol. 188*, 3498−3506.
(44) Ji, H.-F., Shen, L., Carey, J., Grandori, R., and Zhang, H.-Y. (2006) Why WrbA is weaker than flavodoxin in binding FMN. A molecular modeling study. *THEOCHEM 764*, 155−160.
(45) Duax, W. L., Huether, R., Pletnev, V., and Umland, T. C. (2009) Divergent evolution of a Rossmann fold and identification of its oldest surviving ancestor. *Int. J. Bioinf. Res. Appl. 5*, 280−294.
(46) Freigang, J., Diederichs, K., Schafer, K. P., Welte, W., and Paul, R. (2002) Crystal structure of oxidized flavodoxin, an essential protein in *Helicobacter pylori*. *Protein Sci. 11*, 253−261.
(47) Ahn, H. J., Yoon, H. J., Lee, B., II, and Suh, S. W. (2004) Crystal structure of chorismate synthase: A novel FMN-binding protein fold and functional insights. *J. Mol. Biol. 336*, 903−915.